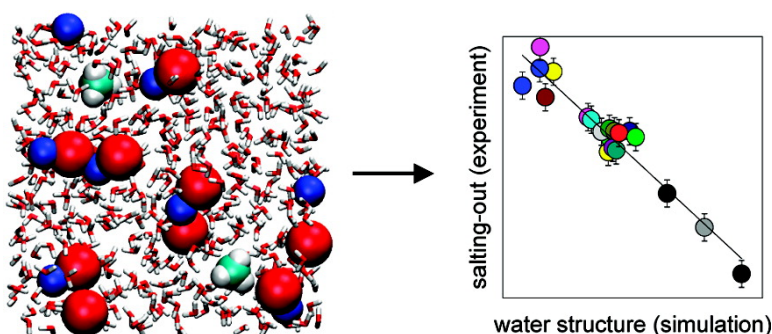


Molecular Dynamics Simulations of Hydrophobic Associations in Aqueous Salt Solutions Indicate a Connection between Water Hydrogen Bonding and the Hofmeister Effect

Andrew S. Thomas, and Adrian H. Elcock

J. Am. Chem. Soc., 2007, 129 (48), 14887-14898 • DOI: 10.1021/ja073097z

Downloaded from <http://pubs.acs.org> on February 9, 2009



More About This Article

Additional resources and features associated with this article are available within the HTML version:

- Supporting Information
- Links to the 9 articles that cite this article, as of the time of this article download
- Access to high resolution figures
- Links to articles and content related to this article
- Copyright permission to reproduce figures and/or text from this article

[View the Full Text HTML](#)



ACS Publications
 High quality. High impact.

Molecular Dynamics Simulations of Hydrophobic Associations in Aqueous Salt Solutions Indicate a Connection between Water Hydrogen Bonding and the Hofmeister Effect

Andrew S. Thomas and Adrian H. Elcock*

Contribution from the Department of Biochemistry, University of Iowa, Iowa City, Iowa 52242

Received May 2, 2007; E-mail: adrian-elcock@uiowa.edu

Abstract: Although the often profound effects of neutral salts on protein solubility were first identified over a century ago by Hofmeister, a general molecular explanation of these effects—capable of accounting even for salts with highly anomalous behavior—has yet to be established. As one way toward developing such an explanation, we aim here to quantify how eight simple monovalent salts alter the association thermodynamics of hydrophobic solute-pairs in a series of 1 μ s explicit-solvent molecular dynamics simulations. For both methane–methane and neopentane–neopentane associations, the salt-induced strengthening of the hydrophobic interaction observed in the simulations is found to be highly correlated with corresponding experimental solubility data; the computed changes in interaction free energy are also found to be quantitatively predictable using the preferential interaction formalism of Timasheff (Timasheff, S. N. *Adv. Protein Chem.* **1998**, *51*, 355–432). From additional simulations of 20 different pure salt solutions—in which no hydrophobic solutes are present—a strong correlation is also observed between the extent of water–water hydrogen bonding and experimental solubility data for hydrophobic solutes; this suggests that the Hofmeister effects of the simple salts investigated here may primarily be a manifestation of salt-induced changes in the water structure. Importantly, all of the strong correlations with experiment obtained here extend even to salts of lithium, whose unusual behavior has previously been unexplained; lithium’s anomalous behavior can be rationalized in part by its formation of alternating, linear clusters (strings) with halide anions. The close agreement between simulation and experiment obtained in the present study reinforces previous work, showing that molecular simulations can be a valuable tool for understanding salt-related phenomena and indicating that this can be so even when the simulations employ the simple, nonpolarizable potential functions widely used in simulations of biological macromolecules.

Introduction

Since aqueous salt solutions form the natural environments for biological macromolecules, it is perhaps not surprising that many important biological processes are sensitive to changes in the concentration and nature of dissolved ions.^{1–3} It is reasonably well-understood that salts can affect electrostatic interactions either through indirect screening of charge–charge interactions⁴ or by direct binding and neutralization of charged groups.⁵ Less well-understood is the mechanism by which salts affect the properties of uncharged or hydrophobic groups in aqueous solution. In Hofmeister’s pioneering works of the late 19th century,^{6,7} it was shown that different salts have widely varying tendencies to alter the aqueous solubilities of egg white proteins; following these initial experiments, qualitatively similar

solubility trends were observed for a wide range of solute types.^{3,8–12} Previous experimental studies exploring the Hofmeister effect—which, it should be noted, has also come to be applied generically to any solute property that is dependent on the specific identity of the salt in solution—have been the subject of a number of comprehensive reviews.^{1–3}

Quantification of the Hofmeister (solubility) effect of a salt is usually obtained via linear regression of the relative solubility of a chosen solute (e.g., proteins, peptides, or simple organic molecules)^{3,8–12} versus the salt’s concentration; the slope of such a correlation is generally termed the Setchenow constant.^{11–13} Although such constants are available for a wide range of salts, and provide useful measures of the salting-in and salting-out behavior of individual types of salt ions, they do not reveal the mechanism by which salts actually modulate solute behavior. Indirect clues can perhaps be obtained from the fact that salt-induced changes in other macroscopic solution properties such as surface tension, viscosity, and osmotic coefficient often

(1) Cacace, M. G.; Landau, E. M.; Ramsden, J. J. *Q. Rev. Biophys.* **1997**, *30*, 241–277.

(2) Collins, K. D.; Washabaugh, M. W. *Q. Rev. Biophys.* **1985**, *18*, 323–422.

(3) von Hippel, P. H.; Schleich, T. In *Structure and Stability of Biological Macromolecules*; Timasheff, S. N., Fasman, G. D., Eds.; Marcel Dekker: New York, 1969; Vol. 2, pp 417–573.

(4) Debye, P.; Hückel, E. *Phys. Z.* **1923**, *24*, 185–206.

(5) Collins, K. D. *Methods* **2004**, *34*, 300–311.

(6) Hofmeister, F. *Arch. Exp. Pathol. Pharmacol.* **1888**, *24*, 247–260.

(7) Kunz, W.; Henle, J.; Ninham, B. W. *Curr. Opin. Colloid Interface Sci.* **2004**, *9*, 19–37.

(8) McDevit, W. F.; Long, F. A. *J. Am. Chem. Soc.* **1952**, *74*, 1773–1777.

(9) Nandi, P. K.; Robinson, D. R. *J. Am. Chem. Soc.* **1972**, *94*, 1308–1315.

(10) Nandi, P. K.; Robinson, D. R. *J. Am. Chem. Soc.* **1972**, *94*, 1299–1308.

(11) Weisenberger, S.; Schumpe, A. *AIChE J.* **1996**, *42*, 298–300.

(12) Xie, W. H.; Shiu, W. Y.; Mackay, D. *Mar. Environ. Res.* **1997**, *44*, 429–444.

(13) Setchenow, J. Z. *Phys. Chem.* **1889**, *4*, 117.

correlate with the Hofmeister (solubility) effects.^{2,14–16} Changes in solution properties largely reflect changes to the behavior of the solvent, in this case water, and it seems reasonable therefore to imagine that salts might influence the solubility of hydrophobic solutes by altering, in some way, the overall liquid water structure. It is, of course, well-known that ions differ widely in their effects on the local water structure:^{17–21} molecular simulations, for example, have shown that small (charge-dense) ions exert strong orientational effects on water molecules within their first solvation shell, severely limiting the latter's abilities to form hydrogen bonds with other water molecules;^{22,23} larger (charge-diffuse) ions on the other hand, appear to behave more like hydrophobic solutes, with their solvating waters in some cases forming more water–water hydrogen bonds than are found in bulk water.^{22,23}

As might be anticipated, therefore, the different effects of charge-dense and charge-diffuse ions on local water structuring are also mirrored, broadly speaking, in their different Hofmeister effects: very charge-dense ions such as Mg^{2+} strongly decrease the aqueous solubility of hydrophobic molecules (Setchenow constant approximately +0.17),¹¹ less charge-dense ions such as Na^+ cause more modest decreases in solubility (Setchenow constant approximately +0.11),¹¹ while ions in which the charge is very diffusely distributed such as $(\text{CH}_3\text{CH}_2)_4\text{N}^+$ may actually increase solubility (Setchenow constant approximately –0.10).^{11,12} A conspicuous exception to this general trend, however, is provided by the behavior of salts containing lithium. Of the Group I cations, Li^+ is the most charge-dense and as such would be expected to cause the greatest salting-out effect and therefore to have the most positive Setchenow constant. However, experimental solubility measurements have shown that for a wide range of solutes, Li^+ 's Setchenow constant is very similar to that of the least charge-dense Group I cation Cs^+ , with Rb^+ , K^+ , and Na^+ all being more effective at salting-out hydrophobic molecules.¹¹ This anomalous behavior¹¹ demonstrates that consideration of the charge densities of salt ions alone is not sufficient to rationalize their Hofmeister effects.⁵

In addition to the studies noted above, a large number of studies have used molecular simulations to explore the behaviors of ions in aqueous solution and/or to attempt to resolve questions about the origins of the Hofmeister effect; since atomically detailed simulations treat all atoms explicitly, they include—in principle—all of the types of interactions that might be necessary for describing the effects of salts on the solubility of biomolecules. The majority of these simulation studies have focused on pure salt solutions and have been primarily aimed at reproducing the hydration thermodynamics of the constituent

ions^{24–28} or correctly describing the structures of their hydration shells.^{15,22,23,25,27,29–44} Other studies have focused on behavior at the vapor–solution interface and have shown that the localization of ions to the interface depends strongly on the nature of the ion;⁴⁵ such studies give insights into surface tension effects,⁴⁶ which as noted previously often correlate with Hofmeister effects.²

The previous studies of pure (i.e., solute-free) aqueous salt solutions provide important groundwork for studying the more complex issue of how solutes, such as hydrophobic molecules, behave when immersed in salt solutions. One way to investigate such behavior is to examine the interaction between an isolated hydrophobic solute and dissolved salts in aqueous solution; a series of molecular simulations focusing on this aspect has been reported by Smith and the results interpreted with Kirkwood–Buff theory,⁴⁷ producing good agreement between computed and experimental Setchenow constants.⁴⁸ A second way to address the effects of dissolved salts on the behavior of hydrophobic solutes—and the approach that is followed in the present work—is to examine how salts alter the thermodynamics of molecular associations between pairs of hydrophobic solutes. Direct quantification of the interaction thermodynamics of hydrophobic solutes such as methane^{34,38,49,50} and amphipathic solutes such as amino acids^{51,52} has been reported for a few select salt solutions (e.g., NaCl) using explicit-solvent simulations. These studies have shown that salts such as NaCl strengthen hydrophobic interactions in a roughly linear manner with the salt concentration, which is consistent with the experimentally observed effects of salts on solubilities.^{11–13} More recently, hydrophobic interactions have also been studied in solutions of artificial ions in a variety of (noninteger) charge states, showing that in general, more charge-dense ions promote hydrophobic aggregation,^{53,54} again, this observation is consis-

- (14) Breslow, R.; Guo, T. *Proc. Natl. Acad. Sci. U.S.A.* **1990**, *87*, 167–169.
 (15) Hribar, B.; Southall, N. T.; Vlachy, V.; Dill, K. A. *J. Am. Chem. Soc.* **2002**, *124*, 12302–12311.
 (16) Kunz, W.; Belloni, L.; Bernard, O.; Ninham, B. W. *J. Phys. Chem. B* **2004**, *108*, 2398–2404.
 (17) Cappa, C. D.; Smith, J. D.; Messer, B. M.; Cohen, R. C.; Saykally, R. J. *J. Phys. Chem. B* **2006**, *110*, 5301–5309.
 (18) Näslund, L. A.; Edwards, D. C.; Wernet, P.; Bergmann, U.; Ogasawara, H.; Pettersson, L. G. M.; Myneni, S.; Nilsson, A. *J. Phys. Chem. A* **2005**, *109*, 5995–6002.
 (19) Omta, A. W.; Kropman, M. F.; Woutersen, S.; Bakker, H. J. *Science (Washington, DC, U.S.)* **2003**, *301*, 347–349.
 (20) Leberman, R.; Soper, A. K. *Nature (London, U.K.)* **1995**, *378*, 364–366.
 (21) Petersen, P. B.; Saykally, R. J. *J. Phys. Chem. B* **2006**, *110*, 14060–14073.
 (22) Dill, K. A.; Truskett, T. M.; Vlachy, V.; Hribar-Lee, B. *Annu. Rev. Biophys. Biomol. Struct.* **2005**, *34*, 173–199.
 (23) Shinto, H.; Morisada, S.; Higashitani, K. *J. Chem. Eng. Jpn.* **2005**, *38*, 465–477.

- (24) Åqvist, J. *J. Phys. Chem.* **1990**, *94*, 8021–8024.
 (25) Chandrasekhar, J.; Spellmeyer, D. C.; Jorgensen, W. L. *J. Am. Chem. Soc.* **1984**, *106*, 903–910.
 (26) Grossfield, A.; Ren, P. Y.; Ponder, J. W. *J. Am. Chem. Soc.* **2003**, *125*, 15671–15682.
 (27) Kalra, A.; Tugcu, N.; Cramer, S. M.; Garde, S. *J. Phys. Chem. B* **2001**, *105*, 6380–6386.
 (28) Rashin, A. A.; Honig, B. *J. Phys. Chem.* **1985**, *89*, 5588–5593.
 (29) Babu, C. S.; Lim, C. *J. Phys. Chem. A* **2006**, *110*, 691–699.
 (30) Chowdhuri, S.; Chandra, A. *J. Chem. Phys.* **2001**, *115*, 3732–3741.
 (31) Degève, L.; Mazze, F. M. *Mol. Phys.* **2003**, *101*, 1443–1453.
 (32) Du, H.; Rasaiah, J. C.; Miller, J. D. *J. Phys. Chem. B* **2007**, *111*, 209–217.
 (33) Gavryushov, S.; Linse, P. *J. Phys. Chem. B* **2006**, *110*, 10878–10887.
 (34) Ghosh, T.; Kalra, A.; Garde, S. *J. Phys. Chem. B* **2005**, *109*, 642–651.
 (35) Grossfield, A. *J. Chem. Phys.* **2006**, *125*, 24506.
 (36) Guardia, E.; Laria, D.; Marti, J. *J. Phys. Chem. B* **2006**, *110*, 6332–6338.
 (37) Jensen, K. P.; Jorgensen, W. L. *J. Chem. Theory Comput.* **2006**, *2*, 1499–1509.
 (38) Jönsson, M.; Skepö, M.; Linse, P. *J. Phys. Chem. B* **2006**, *110*, 8782–8788.
 (39) Kinoshita, M.; Hirata, F. *J. Chem. Phys.* **1997**, *106*, 5202–5215.
 (40) Lyubartsev, A. P.; Laaksonen, A. *Phys. Rev. E* **1995**, *52*, 3730–3737.
 (41) Obst, S.; Bradaczek, H. *J. Phys. Chem.* **1996**, *100*, 15677–15687.
 (42) Patra, M.; Karttunen, M. *J. Comput. Chem.* **2004**, *25*, 678–689.
 (43) Piquemal, J. P.; Perera, L.; Cisneros, G. A.; Ren, P. Y.; Pedersen, L. G.; Darden, T. A. *J. Chem. Phys.* **2006**, *125*, 54511.
 (44) Rajamani, S.; Ghosh, T.; Garde, S. *J. Phys. Chem. B* **2004**, *120*, 4457–4466.
 (45) Vrba, L.; Mucha, M.; Minofar, B.; Jungwirth, P.; Brown, E. C.; Tobias, D. J. *Curr. Opin. Colloid Interface Sci.* **2004**, *9*, 67–73.
 (46) Jungwirth, P.; Tobias, D. J. *Chem. Rev.* **2006**, *106*, 1259–1281.
 (47) Kirkwood, J. G.; Buff, F. P. *J. Chem. Phys.* **1951**, *19*, 774–777.
 (48) Smith, P. E. *J. Phys. Chem. B* **1999**, *103*, 525–534.
 (49) Ghosh, T.; Garcia, A. E.; Garde, S. *J. Phys. Chem. B* **2003**, *107*, 612–617.
 (50) Fujita, T.; Watanabe, H.; Tanaka, S. *Chem. Phys. Lett.* **2007**, *434*, 42–48.
 (51) Hassan, S. A. *J. Phys. Chem. B* **2005**, *109*, 21989–21996.
 (52) Thomas, A. S.; Elcock, A. H. *J. Am. Chem. Soc.* **2006**, *128*, 7796–7806.
 (53) Zangi, R.; Berne, B. J. *J. Phys. Chem. B* **2006**, *110*, 22736–22741.
 (54) Zangi, R.; Hagen, M.; Berne, B. J. *J. Am. Chem. Soc.* **2007**, *129*, 4678–4686.

tent with the general, but imperfect, trend described previously between a salt ion's charge density and its effect on solubility.

Here, we present a relatively comprehensive set of molecular dynamics (MD) simulations aimed at investigating (a) the thermodynamics of hydrophobic interactions in a range of salt solutions that exert weak to moderate Hofmeister effects¹¹ and (b) the connection between observed thermodynamics and measurable structural properties of the solute–solvent systems. We begin by showing that when simulations of hydrophobic associations are performed using off-the-shelf nonpolarizable potential functions, surprisingly good agreement can be obtained with experimentally measured Setchenow constants, even in the case of the anomalously behaving lithium salts. From an analysis of the simulation snapshots, we show that the effects of different salts on hydrophobic associations can be quantitatively rationalized within the context of the preferential interaction (PI) formalism,⁵⁵ but we also proceed to show that the qualitative effects can be equally well-understood from examining the behavior of pure salt solutions (i.e., from simulations that do not directly include any hydrophobic solutes). The latter conclusion stems from an examination of water structuring in 20 different salt solutions comprised of both Group I and Group II cations. The combined simulation time of the study amounts to $\sim 26 \mu\text{s}$ and demonstrates that a near-quantitative understanding of the weak to moderate Hofmeister effects of the simple salts used in this study can be obtained using currently available simulation forcefields and methodologies.

Materials and Methods

MD Simulations. MD simulations were performed using GRO-MACS software.^{56,57} All monatomic salt ions were modeled using parameters developed by others^{24,25,58,59} and implemented in GRO-MACS; the more complex ammonium and tetra-alkyl ammonium ions were modeled using parameters derived from the OPLS-AA parameters for protonated lysine⁶⁰ (see Supporting Information). Water was described throughout by the TIP3P model,⁶¹ and hydrophobic solutes were modeled with the OPLS-AA forcefield⁶² implemented in GRO-MACS. Simulations were performed within a $25 \text{ \AA} \times 25 \text{ \AA} \times 25 \text{ \AA}$ box to which periodic boundary conditions were applied; systems therefore were comprised of approximately 500 water molecules. In all cases, ions were initially placed randomly within the simulation box; for simulations of methane pairs and neopentane pairs, the two hydrophobic solutes were initially separated by 10 \AA (rapid equilibration of the systems ensured that results were insensitive to the initial placement of ions and hydrophobic solutes). Systems were first energy minimized with a steepest descent minimization for 100 steps, gradually heated to 298 K over the course of 500 ps, and then equilibrated for a further 10 ns. Following this point, production simulations were performed with the temperature maintained at 298 K using the Nosé–Hoover thermostat,^{63,64} and the pressure was maintained at 1 atm using

the Parrinello–Rahman barostat.⁶⁵ A 2 fs time step was used in all simulations with all bonds being constrained to their equilibrium lengths using the LINCS algorithm.⁶⁶ A cutoff of 10 \AA was applied to short-range nonbonded interactions, and the PME method⁶⁷ was used to calculate all long-range electrostatic interactions.

Systems Studied. Essentially, three separate simulation studies were conducted. In the first, systems containing pairs of methane molecules or neopentane molecules were simulated in 1 M solutions of the following salts: LiCl, LiBr, NaF, NaCl, NaBr, KF, KCl, and KBr (LiF was also simulated, but the salt rapidly crystallized from solution, consistent with experiment⁶⁸). Each of these systems was simulated for 1 μs to obtain statistically converged estimates of the association thermodynamics of the hydrophobic solutes. In a second set of simulations, the association thermodynamics of the same hydrophobic pairs were examined in NaCl solutions of the following concentrations: 0.1, 0.3, 0.5, 1, and 2 M; each of these systems was simulated for 500 ns. Finally, in a third set of simulations, 20 pure 1 M salt solutions (i.e., containing no hydrophobic solutes) were each simulated for 100 ns to obtain converged views of the effects of these salts on water structuring and their tendencies to form ion clusters. For this latter study, the following salts were simulated: LiCl, LiBr, LiI, NaF, NaCl, NaBr, NaI, KF, KCl, KBr, KI, RbCl, CsCl, NH_4Cl , NH_4Br , MgCl_2 , CaCl_2 , BaCl_2 , $(\text{CH}_3)_4\text{NBr}$, and $(\text{CH}_3\text{CH}_2)_4\text{NBr}$. In all simulations, system snapshots (comprised of all atoms) were collected every 0.1 ps for subsequent analysis. Error estimates for all simulation observables were obtained from the standard deviation of the observable calculated when the full trajectory was split into five equal length blocks.

Computation of Molecular Association Thermodynamics. For systems containing hydrophobic solute-pairs, excess (interaction) free energies as a function of the distance between the two solutes were obtained from histograms of the intermolecular distance sampled during the simulations; the methods used have been described in detail in previous work.^{52,69,70}

Analysis of Water Hydrogen Bonding. To assess the effects of dissolved salts on liquid water structure in the simulations, three different measures were used. The first was the familiar water oxygen–oxygen radial distribution function (RDF), which describes the spherically averaged distribution of oxygen–oxygen separation distances between pairs of water molecules sampled from the simulation trajectory. Since this RDF is only a function of the oxygen–oxygen separation distance, it does not explicitly describe hydrogen bonding, which, as might be expected, is better represented by RDFs of oxygen–hydrogen distances; this therefore was the second measure used to describe water structuring. Finally, to more directly describe water–water hydrogen bonding, and to quantify the extent of water structuring at discrete distances from individual ions, a third measure was calculated as follows. For every water molecule in the system, the number of neighboring water molecules, N_{ngbr} , for which the oxygen–oxygen distance was $< 3.5 \text{ \AA}$ was first computed. Next, the number of these neighbors that formed a hydrogen bond to the central water molecule was determined (N_{hbnds}); this was decided by applying the conventional geometric criterion that the $\text{H–O}\cdots\text{O}$ angle be $< 30^\circ$ (alternative definitions exist,⁷¹ but the results we report here are insensitive to the exact definition chosen). We then defined our third measure of water structuring (which we denote θ_{hb}) as $\theta_{\text{hb}} = N_{\text{hbnds}}/N_{\text{ngbr}}$. θ_{hb} has an upper limit of 1, which is achieved when all neighboring water molecules form hydrogen bonds to the central (reference) water

(55) Arakawa, T.; Timasheff, S. N. *Biochemistry* **1982**, *21*, 6545–6552.

(56) Lindahl, E.; Hess, B.; van der Spoel, D. *J. Mol. Model.* **2001**, *7*, 306–317.

(57) Van der Spoel, D.; Lindahl, E.; Hess, B.; Groenhof, G.; Mark, A. E.; Berendsen, H. J. C. *J. Comput. Chem.* **2005**, *26*, 1701–1718.

(58) Lybrand, T. P.; Ghosh, I.; McCammon, J. A. *J. Am. Chem. Soc.* **1985**, *107*, 7793–7794.

(59) McDonald, N. A.; Duffy, E. M.; Jorgensen, W. L. *J. Am. Chem. Soc.* **1998**, *120*, 5104–5111.

(60) Kaminski, G. A.; Friesner, R. A.; Tirado-Rives, J.; Jorgensen, W. L. *J. Phys. Chem. B* **2001**, *105*, 6474–6487.

(61) Jorgensen, W. L.; Chandrasekhar, J.; Madura, J. D.; Impey, R. W.; Klein, M. L. *J. Chem. Phys.* **1983**, *79*, 926–935.

(62) Jorgensen, W. L.; Maxwell, D. S.; Tirado-Rives, J. *J. Am. Chem. Soc.* **1996**, *118*, 11225–11236.

(63) Hoover, W. G. *Phys. Rev. A* **1985**, *31*, 1695–1697.

(64) Nosé, S. *J. Chem. Phys.* **1984**, *81*, 511–519.

(65) Parrinello, M.; Rahman, A. *J. Appl. Phys.* **1981**, *52*, 7182–7190.

(66) Hess, B.; Bekker, H.; Berendsen, H. J. C.; Fraaije, J. G. E. M. *J. Comput. Chem.* **1997**, *18*, 1463–1472.

(67) Essmann, U.; Perera, L.; Berkowitz, M. L.; Darden, T.; Lee, H.; Pedersen, L. G. *J. Chem. Phys.* **1995**, *103*, 8577–8593.

(68) Collins, K. D. *Biophys. J.* **1997**, *72*, 65–76.

(69) Thomas, A. S.; Elcock, A. H. *J. Am. Chem. Soc.* **2004**, *126*, 2208–2214.

(70) Yang, H. B.; Elcock, A. H. *J. Am. Chem. Soc.* **2003**, *125*, 13968–13969.

(71) Kumar, R.; Schmidt, J. R.; Skinner, J. L. *J. Chem. Phys.* **2007**, *126*, 204107.

molecule, and a lower limit of 0, achieved when none of the neighboring water molecules forms a hydrogen bond to the central water molecule. It should be noted that very similar quantities have been used by others previously to describe water structuring around ions^{23,41} and hydrophobic solutes.³⁸ The mean values of θ_{hb} reported in the Results are averages of the θ_{hb} values computed for all water molecules during the final 20 ns of each 100 ns simulation (see the previous discussion for an explanation of the simulation lengths).

Ion–Solute Preferential Interactions. As an aid to rationalizing the effects of salts on the computed association thermodynamics, we have employed the PI formalism⁵⁵ via a procedure identical to that described previously by Garde and co-workers;³⁴ this approach was chosen in place of an alternative approach outlined by Smith⁴⁸ since it has already been shown to be easily applied to the study of association reactions. The preferential interaction parameter of each salt, Γ_{salt} , was determined independently for the hydrophobic solute pairs in their associated and dissociated states by separating snapshots from the MD simulations based on the inter-solute distance. For the methane–methane system, snapshots were considered to be representative of the associated state if the methane–methane separation was between 3.8 and 4.0 Å, while snapshots were considered to be representative of the dissociated state if the methane–methane separation was between 12.2 and 12.8 Å (this separation distance being the most extensively sampled in the simulations). For the neopentane–neopentane system, the corresponding distance ranges were 5.6–5.8 and 15.5–16.0 Å, respectively.

The difference in the computed Γ_{salt} values [$\Delta\Gamma_{\text{salt}} = \Gamma_{\text{salt}}(\text{dissociated}) - \Gamma_{\text{salt}}(\text{associated})$]³⁴ gives a measure of a salt's preference for interacting with the hydrophobic solutes in a dissociated versus an associated state: negative values indicate that the salt prefers to interact with the associated state and therefore favors the association (i.e., aggregation) of the hydrophobic solutes. As noted by Garde and colleagues,³⁴ the exact values of Γ_{salt} and $\Delta\Gamma_{\text{salt}}$ that are obtained with their formalism depend on the cutoff distance that is used to determine whether a salt ion is bound to either of the two hydrophobic solutes; however, in this work, the same qualitative trends of $\Delta\Gamma_{\text{salt}}$ values for the various salts were obtained regardless of the cutoff definition. For specific comparisons with experimental data shown in the Results, the cutoff distance was chosen separately for each salt by identifying the region on the plot of $\Delta\Gamma_{\text{salt}}$ versus the cutoff distance where the curve reaches its first minimum: this use of a variable cutoff distance simply accounts for the fact that different ions have different radii and so will naturally have different preferred distances for binding to the hydrophobic solutes. The different definitions of the cutoff distances used, and plots showing how the computed $\Delta\Gamma_{\text{salt}}$ values change when different fixed cutoff distances are used, are all shown in the Supporting Information.

Since the emphasis of the current work is on understanding the effects of salt on hydrophobic associations, our primary interest is in our computed $\Delta\Gamma_{\text{salt}}$ values (see Results). It has, however, been rightly pointed out by an anonymous reviewer that the absolute Γ_{salt} values are themselves also of interest. In particular, it is to be anticipated that the Γ_{salt} values computed for different salts should correlate with their experimental Setchenow constants: the latter measure is, after all, usually employed to describe the relative solubilities of nonpolar gases that, given their low solubilities, may be considered to be unassociated with one another. In fact, we do indeed find a good correlation: the Γ_{salt} values computed for the dissociated states correlate with the corresponding Setchenow constants with $r^2 = 0.929$ for methane and $r^2 = 0.935$ for neopentane (Figure S1).

Results

Simulations of Hydrophobic Solutes in Salt Solutions. The effective interaction free energies of pairs of hydrophobic solutes were calculated from 1 μs MD simulations of the pairs in water and eight different 1 M alkali metal halide solutions. As is

commonly seen for hydrophobic associations in water,^{34,72} all free energy curves show three favorable minima: for methane pairs (Figure 1a), a strong direct solute–solute contact is observed at ~ 3.8 Å, a weaker solvent-separated configuration involving a single water layer is observed at ~ 7.2 Å, and a barely discernible solvent-separated configuration involving a double water layer is observed at ~ 10.3 Å; similar free energy minima are also observed with neopentane pairs but occur at separations that are ~ 2 Å further apart than those observed with methane pairs (Figure 1b). Close-up views of the direct contact free energy minima for both pairs of hydrophobic solutes (insets of Figure 1a,b) highlight the differences in the free energy of interaction in different salt solutions. As has been noted previously from studies of methane–methane association in NaCl solutions,^{34,50} similar qualitative salt trends are also observed for the solvent-separated minima and maxima, suggesting that salts affect all configurations of hydrophobic association in a qualitatively similar manner. This can be seen most clearly when the free energies of interaction in the salt solutions are plotted—relative to their values in pure water—versus the inter-solute distance (Figure S2).

For all eight salts studied, the addition of salt strengthens the hydrophobic interaction in the simulations; our results for NaCl are broadly consistent with those obtained previously by others.^{34,38,50,52} For both the methane–methane interaction and the neopentane–neopentane interaction, the strongest stabilizing effects are caused by the two fluoride salts studied (KF and NaF), while the weakest stabilizing effects are caused by the two lithium salts (LiBr and LiCl). Two points are especially worth noting. First, the trends observed in these MD simulations turn out to be in very good agreement with the experimentally measured Setchenow (salting-out) constants for the same salts: linear regressions of the depth of the direct contact free energy minimum with the experimental Setchenow constants (Figure 1c,d) produce strong correlations for both the methane–methane ($r^2 = 0.780$) and the neopentane–neopentane ($r^2 = 0.863$) interactions (these correlations can be further improved by the addition of the extra data point from pure water simulations). The somewhat better quality of fit observed for the neopentane pair is probably due to its greater sensitivity to salt: consistent with the experimental finding that the magnitude of the experimental Hofmeister effect is greater for larger hydrophobic solutes,¹¹ the contact minimum for the neopentane pair is stabilized by 0.19 kcal/mol upon the addition of 1 M KF, while the corresponding minimum for the methane pair is stabilized by only 0.12 kcal/mol. The second important point to note is the simulations' correct identification of Li^+ as the cation with the weakest stabilizing effect of the three cations studied: as is explored in more detail next, the rank ordering of stabilization effects that is obtained ($\text{Li}^+ < \text{K}^+ < \text{Na}^+$) is the same as that observed experimentally.¹¹ Since, as noted in the Introduction, Li^+ 's behavior is impossible to rationalize on the basis of its charge density alone,¹⁵ this result demonstrates that the MD simulations are capable of correctly reproducing salt-dependent behavior that is not at all trivial to capture.

To rationalize the trends obtained above, we begin by examining possible interactions between salt ions and hydrophobic solutes and attempt to quantify their effects on the

(72) Lee, M. E.; van der Vegt, N. F. A. *J. Am. Chem. Soc.* **2006**, *128*, 4948–4949.

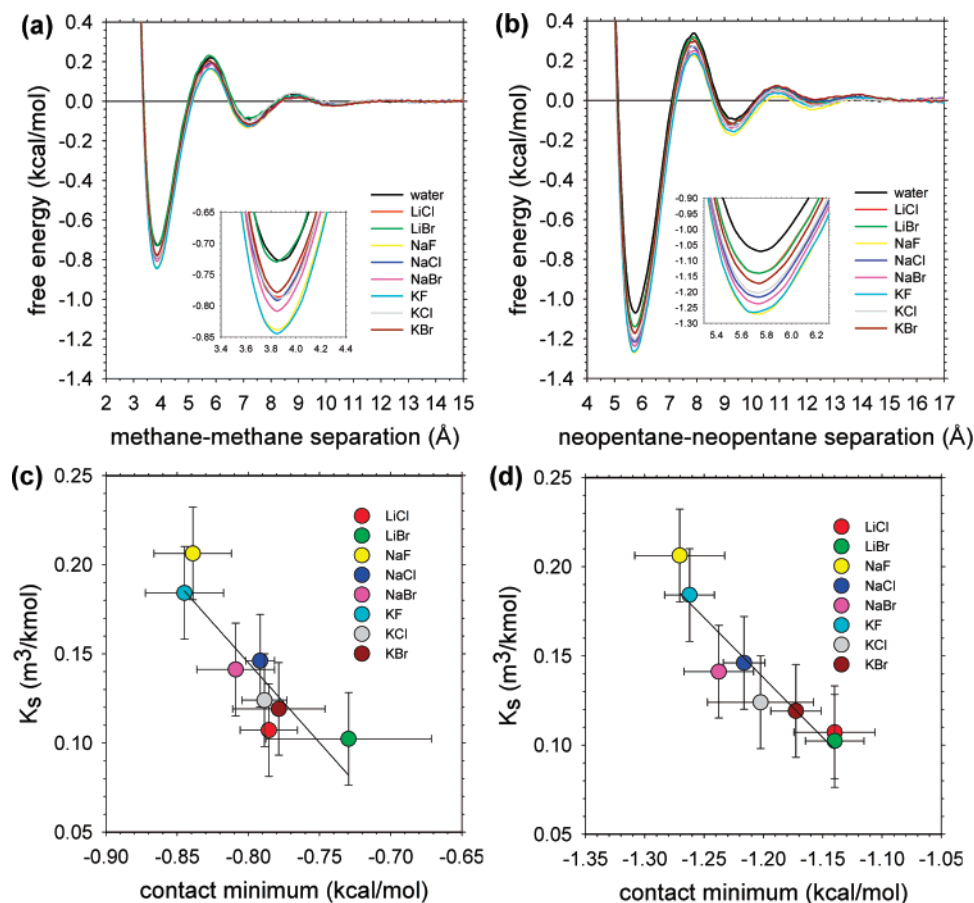


Figure 1. Salt effects on hydrophobic interactions. (a) Free energy of interaction for a pair of methane molecules as a function of their separation in different salt solutions; inset shows a close-up of the contact free energy minimum. The average uncertainty in all plots is 3.5% or 0.025 kcal/mol at the contact free energy minimum. (b) Free energy of interaction for a pair of neopentane molecules in different salt solutions; inset shows a close-up of the contact free energy minimum. The average uncertainty for all plots is 2.5% or 0.030 kcal/mol at the contact free energy minimum. (c) Experimental Setchenow constants vs free energy of the contact minimum for the methane–methane pair ($r^2 = 0.780$). (d) Experimental Setchenow constants vs free energy of the contact minimum for the neopentane–neopentane pair ($r^2 = 0.863$). The experimental data (and their error bars) are taken from ref 11.

thermodynamics of the hydrophobic association. To do this, we make use of the PI formalism developed by Timasheff, Record, and others;^{34,73,74} by applying the formalism separately to simulation snapshots representative of the associated and dissociated states and calculating the difference, $\Delta\Gamma_{\text{salt}}$, we can obtain a direct connection between changes in the distribution of ions and changes in the observed association thermodynamics. We find that those salts that most strengthen the hydrophobic interactions (NaF and KF)—as judged from the changes in computed free energies of interaction (Figure 1a,b)—also produce the most negative values of $\Delta\Gamma_{\text{salt}}$ (see Table 1 in Supporting Information for all individual Γ_{salt} and $\Delta\Gamma_{\text{salt}}$ values), indicating that they interact more favorably with the hydrophobic solutes when the latter are in an associated state than when they are in a dissociated state (Figure 2a,b). Similarly, we find that the salt that strengthens hydrophobic interactions the least (LiBr; Figure 1a,b) produces the least negative value of $\Delta\Gamma_{\text{salt}}$ (Figure 2a,b). As noted in the Materials and Methods, the computed values of $\Delta\Gamma_{\text{salt}}$ that are obtained depend on a cutoff distance that is used to determine whether an ion is bound to the hydrophobic solutes; as can be seen from Figure 2a,b, however,

the rank ordering of the salts that is obtained is largely independent of the chosen cutoff distance.³⁴ The only exception to this rule is LiCl, which, for both methane–methane and neopentane–neopentane systems, changes from having the second-most positive $\Delta\Gamma_{\text{salt}}$ value when a cutoff distance of 5 Å is used to having the sixth-most positive $\Delta\Gamma_{\text{salt}}$ value when a (probably less physically meaningful) cutoff distance of 10 Å is used. The reasons for the latter behavior are not obvious but are perhaps most likely due to sampling issues: as is described in detail next, lithium salts tend to form strings of ions, which may limit our ability to fully sample their spatial distributions around the hydrophobic solutes. Regardless of the cutoff distance chosen, however, we find that the computed $\Delta\Gamma_{\text{salt}}$ values correlate very well with experimental Setchenow constants (Figure 2c; $r^2 = 0.949$ and $r^2 = 0.943$ for methane and neopentane pairs, respectively); Figure S3 shows that the correlations remain very good when different cutoff distances are used.

Perhaps more importantly, the magnitudes of the $\Delta\Gamma_{\text{salt}}$ values also provide an excellent indication of the quantitative effect of a salt on the computed association thermodynamics of the two different solute types studied: the $\Delta\Gamma_{\text{salt}}$ values for the neopentane–neopentane interaction are $\sim 40\%$ more negative than those for the methane–methane interaction (compare Figure 2a,b), which is consistent with the fact that the salt-

(73) Record, M. T.; Zhang, W. T.; Anderson, C. F. *Adv. Protein Chem.* **1998**, *51*, 281–353.

(74) Timasheff, S. N. *Adv. Protein Chem.* **1998**, *51*, 355–432.

(75) Humphrey, W.; Dalke, A.; Schulten, K. *J. Mol. Graphics* **1996**, *14*, 33–38.

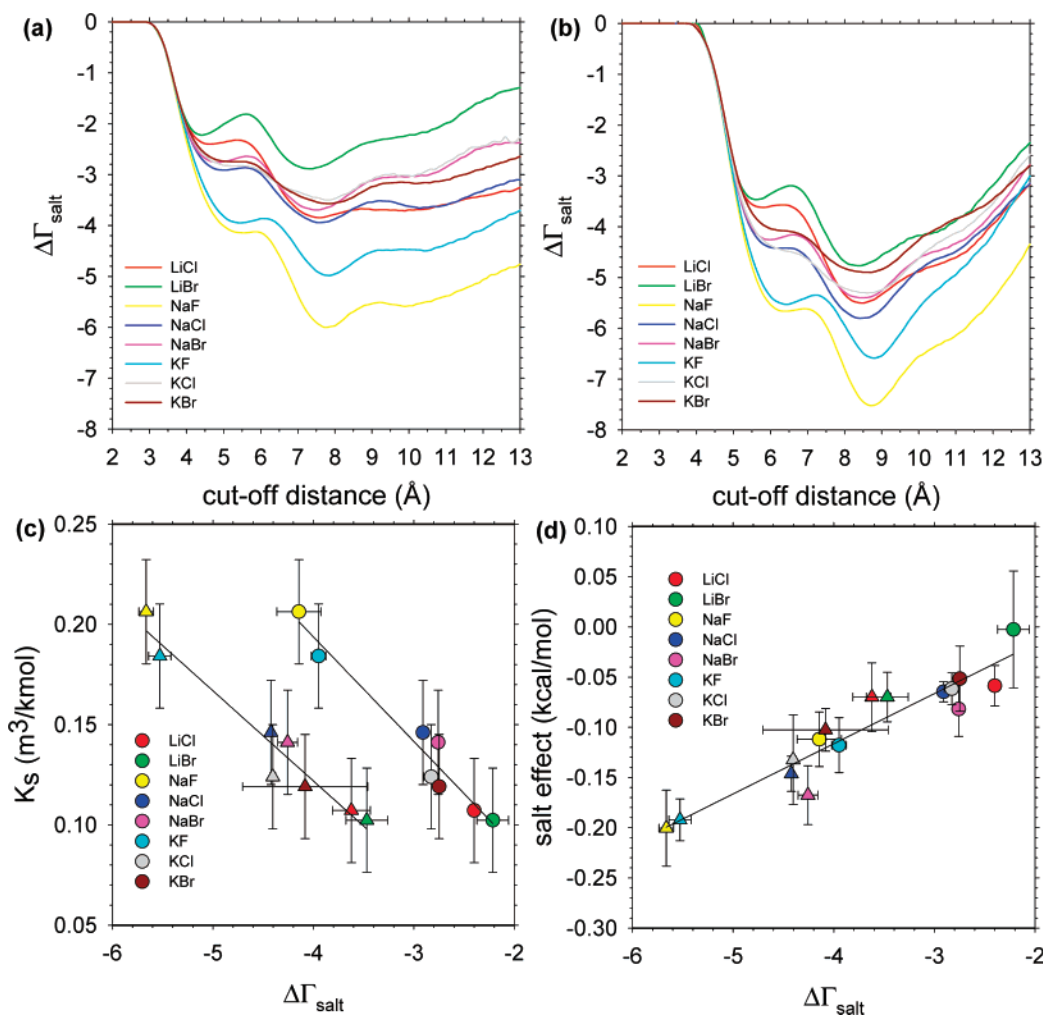


Figure 2. Changes in salt preferential interaction coefficient ($\Delta\Gamma_{\text{salt}}$) upon dissociation of hydrophobic solute pairs. (a) $\Delta\Gamma_{\text{salt}}$ for methane pairs in salt solutions plotted vs the cutoff distance used to determine whether ions are bound to the solutes (see Materials and Methods). (b) $\Delta\Gamma_{\text{salt}}$ for neopentane pairs in salt solutions plotted vs the cutoff distance. (c) Experimental Setchenow constants plotted vs $\Delta\Gamma_{\text{salt}}$ using cutoff distances corresponding to the first minimum from panels a and b for the methane pair (circles, $r^2 = 0.949$) and the neopentane pair (triangles, $r^2 = 0.943$). (d) Change in free energy of interaction at the contact minimum due to addition of a salt plotted vs $\Delta\Gamma_{\text{salt}}$ using the cutoff distance corresponding to the first minimum from panels a and b for the methane pair (circles) and the neopentane pair (triangles) ($r^2 = 0.888$).

dependent stabilization of the contact minimum is typically $\sim 40\%$ greater for the neopentane pair (see Figure 1). In fact, when the computed changes in interaction free energy at the contact minimum due to the addition of salt are plotted against the computed $\Delta\Gamma_{\text{salt}}$ values, the data points obtained from the methane–methane and neopentane–neopentane simulations all fall on a single regression line (Figure 2d, $r^2 = 0.888$). The relatively high quality of this fit suggests that it should be possible to use the PI formalism to quantitatively predict the effect of a salt on the association thermodynamics of any chosen pair of hydrophobic solutes, by performing only two, comparatively short, MD simulations: one simulation with the solutes held in an associated state and one simulation with the solutes held in a dissociated state (e.g., at a separation of ~ 12 – 15 Å).

Simulations of Pure Salt Solutions. While the above results demonstrate that the PI formalism is likely to be a powerful method for rapidly predicting the effects of salts on the association thermodynamics of arbitrary solutes, we were curious, given the ideas presented in the Introduction, as to whether the Hofmeister behavior of a salt might also be predictable using a still simpler approach: by examining the water-structuring behavior of the pure salt solution (i.e., in the

absence of any other dissolved solutes). To explore this question, we selected 20 pure salt solutions (see Materials and Methods), chosen so that they contained both strong salting-out and strong salting-in salts, and performed 100 ns simulations of each of them at a 1 M salt concentration (i.e., at a sufficiently high concentration that observable changes in the water structure might be obtained).

Three different ways of measuring the extent of water structuring in the salt solutions were investigated: the water oxygen–oxygen RDF, the water oxygen–hydrogen RDF, and the mean water–water hydrogen bonding fraction (θ_{hb} ; defined in Materials and Methods). Interestingly, when these three measures are applied to the 20 salts studied, they all produce some degree of correlation with the corresponding experimental Setchenow constants. Perhaps not surprisingly, the measure that provides the least direct description of water–water hydrogen bonding—the water oxygen–oxygen RDF—produces the worst correlation: although the height of the major peak in this RDF correlates with the Setchenow constants nicely for the Group I metal salts, it fails completely for the Group II metal salts (Figure S4). In contrast, the more direct measures of hydrogen bonding—the water oxygen–hydrogen RDF and the

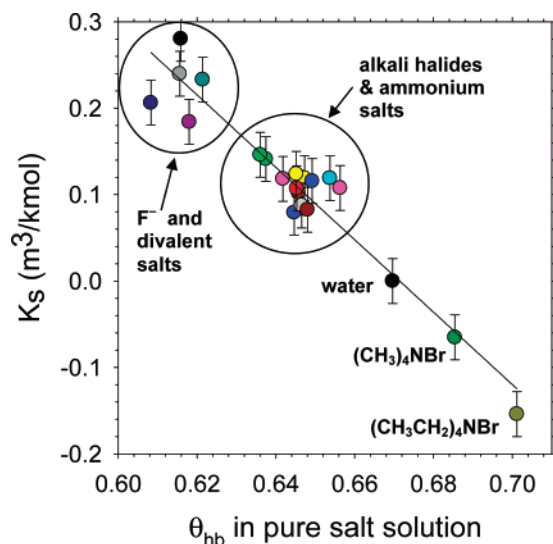


Figure 3. Experimental Setchenow constants and water–water hydrogen bonding. Plot of experimental Setchenow constants vs computed water–water hydrogen bonding fraction (θ_{hb}) obtained from simulations of 1 M salt solutions. Linear regression $r^2 = 0.920$. Experimental error bars taken from ref 11; error bars for θ_{hb} are within the symbol size.

θ_{hb} value—correlate well with the experimental Setchenow constants for all of the salts studied (Figures 3 and S5). As noted in the Materials and Methods, θ_{hb} has the advantage that it can yield a single, readily converged value for individual water molecules and can therefore easily be used to assess how water–water hydrogen bonding properties vary with distance from chosen solutes; consequently, this is the measure that we used for all subsequent analyses.

The relationship that we find between the mean θ_{hb} value of a salt solution and the experimental Hofmeister effect of the salt is straightforward: strongly salting-out salts, such as Group II cation salts or metal fluorides, cause significant decreases in the θ_{hb} value from the pure water value of 0.670 (indicating that water–water hydrogen bonding is diminished), while salting-in salts, such as $(\text{CH}_3\text{CH}_2)_4\text{NBr}$, cause increases in the mean θ_{hb} value (see Table 2 in the Supporting Information for all θ_{hb} values). The high degree of correlation ($r^2 = 0.920$) between the computed θ_{hb} values and the experimental Setchenow constants indicates therefore that it is possible to qualitatively predict the Hofmeister behavior of a salt from a simple examination of its effect on water structure in the absence of any dissolved organic solutes; data showing that this relationship between θ_{hb} and Setchenow constants is unaffected by the addition of hydrophobic solutes are provided in the Supporting Information (Figure S6).

The validity of the proposed connection between water–water hydrogen bonding, as measured by the computed θ_{hb} value of a pure salt solution, and the Hofmeister effect of the same salt can be evaluated in two further ways. First, as might be expected given the good agreement shown earlier between computed free energies of interaction of hydrophobic solute-pairs and experimental Setchenow constants (Figure 1c,d), we find a strong linear correlation between the computed θ_{hb} values of the eight Group I halide salt solutions and the effects of the same salts on the free energies of interaction of both methane–methane ($r^2 = 0.778$) and neopentane–neopentane pairs ($r^2 = 0.836$) (Figure 4a). Second, from additional simulations performed to investigate the sensitivity of the free energies of interaction to

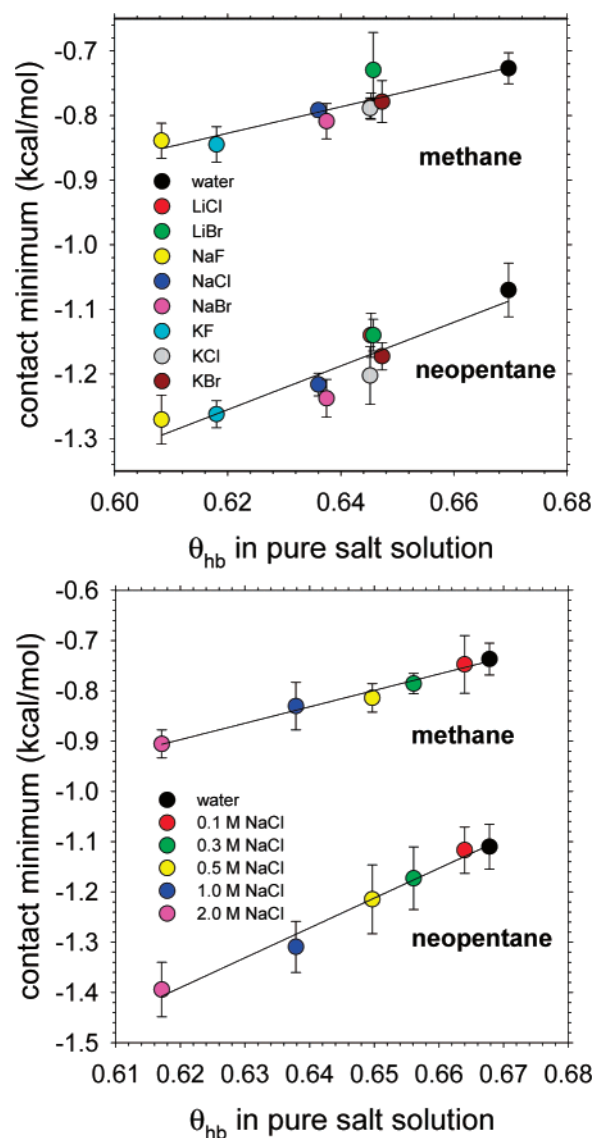


Figure 4. Computed thermodynamics of association and water–water hydrogen bonding. (a) Direct contact free energy minima obtained from 1 μs simulations of methane and neopentane pairs plotted vs mean θ_{hb} values computed from corresponding simulations of pure (hydrophobic solute-free) salt solutions; for the methane pair, $r^2 = 0.778$; for the neopentane pair, $r^2 = 0.836$. (b) Direct contact free energy minima obtained from 500 ns simulations of methane and neopentane pairs in NaCl solutions of different concentrations plotted vs mean θ_{hb} values computed from corresponding simulations of pure (hydrophobic solute-free) NaCl solutions; for the methane pair, $r^2 = 0.982$; for the neopentane pair, $r^2 = 0.984$.

changes in salt concentration (see Materials and Methods), we also find that the computed θ_{hb} values of pure NaCl solutions of concentrations ranging from 0.1 to 2 M strongly correlate with the free energies of interaction of both methane–methane ($r^2 = 0.982$) and neopentane–neopentane ($r^2 = 0.984$) pairs in the same NaCl solutions (Figure 4b). Regardless therefore of whether one examines the effects of different salts at a single concentration (Figure 4a), or the effects of a single salt at different concentrations (Figure 4b), the same qualitative result is obtained: the θ_{hb} value of the pure salt solution correlates with the effect of the salt on the strength of the hydrophobic interactions.

Anomalous Behavior of Lithium Salts. An important point to note in the above analysis is that, in common with the free energies of interaction discussed earlier, the general

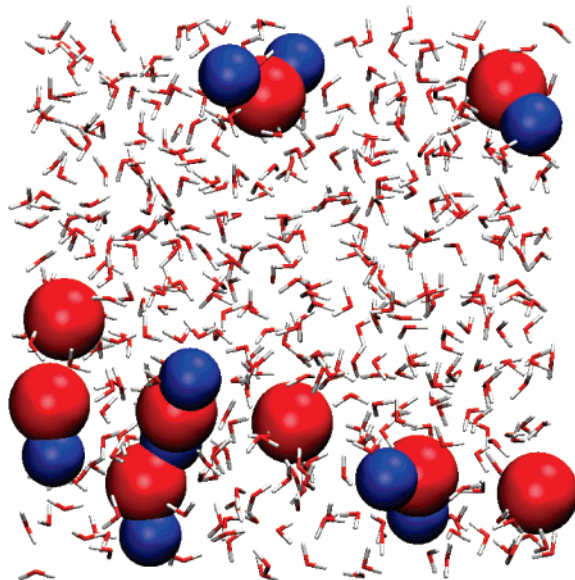


Figure 5. Snapshot from a LiCl simulation showing clusters of Li^+ (blue) and Cl^- (red) ions; this figure was prepared with the program VMD.⁷⁵

correlation that we find between the extent of water–water hydrogen bonding and the experimental Setchenow constants applies equally well to the anomalously behaving lithium salts: a closer analysis of the simulations should therefore allow us to explain why it is that Li^+ 's behavior deviates so markedly from expectations based on the behavior of the other Group I cations. One potential cause of Li^+ 's unusual position in the Hofmeister series can be readily identified from a visual inspection of the simulations: solutions of LiCl (and other lithium salts) show a pronounced tendency to form linear clusters (strings) of ions (Figure 5). In fact, in the lithium halide systems studied, typically 60–70% of the Li^+ ions are directly coordinated with anions during the simulations; in contrast, all other Group I cations remain predominantly dissociated in solution (see Table 3 in the Supporting Information for complete data on ion clustering). As detailed below, a second (related) factor appears to be a comparatively high degree of water–water hydrogen bonding observed around Li^+ ions, a finding that was uncovered by examining the mean θ_{hb} values of water molecules as a function of their distance from the nearest ion in solution. Figure 6 shows the results of such an analysis conducted on the water molecules in pure solutions of the Group I chloride salts: LiCl, NaCl, KCl, RbCl, and CsCl; Figure 6a shows the results for all water molecules whose nearest ion is a cation, while Figure 6b shows the results for all water molecules whose nearest ion is an anion. Examining the less interesting Figure 6b first, there are two points to consider. First, it can be seen that water molecules that are separated by more than 7 Å from a Cl^- have mean θ_{hb} values that are essentially identical to that of bulk water (shown by the horizontal dotted line in Figure 6b), whereas water molecules that lie within the first solvation shell of the Cl^- ion have θ_{hb} values that are decreased somewhat from the bulk value. The former observation is consistent with experiments showing that ions do not substantially affect bulk water behavior even in very concentrated salt solutions;^{17–19} the latter observation is consistent with experiments (and simulation studies) indicating that the water–water hydrogen bonding abilities of water molecules directly coordinating ions are significantly perturbed.^{17–21,23,41} The second point to note

from Figure 6b is that the plots all superimpose more or less directly upon each other; this indicates that the behavior of water molecules around the Cl^- ion is largely insensitive to the nature of the cation partner in the solution. This result, which is also generally true of other comparisons that we have performed (see Figure S7), is consistent with the fact that the Setchenow constant of a salt can usually be well-described as a sum of independent contributions from its constituent cation and anion.¹¹

Examining Figure 6a, which shows the behavior of water molecules whose nearest neighboring ion is a cation, more interesting trends are observed. Focusing on the behavior of water molecules that are closest to the cation, a naïve expectation would be that water–water hydrogen bonding would be drastically weakened in the solvation shell of the smaller ions (since their stronger ion–water interactions should disrupt the ability of the waters to hydrogen bond with each other) but only moderately weakened, if at all, in the first solvation shell of the larger, less charge-dense ions such as Cs^+ . For the most part, this expectation is met: beginning with Cs^+ and ending with Na^+ , there is a monotonic decrease in the degree of water–water hydrogen bonding immediately adjacent to the cation (see distances less than 3 Å in Figure 6a). The trend, however, is reversed with Li^+ (solid red line in Figure 6a): in contrast to expectations, the extent of water–water hydrogen bonding in Li^+ 's first solvation shell (1.8–2.2 Å) is found to be slightly greater than that in Na^+ 's first solvation shell. This indicates that the extent of water–water hydrogen bonding around Li^+ ions is anomalous in comparison to the other Group I cations.

This analysis can be taken a stage further by splitting the mean computed θ_{hb} value into separate contributions from hydrogen bonds that are accepted by each water molecule and hydrogen bonds that are donated by each water molecule. As is to be expected, water molecules in the first solvation shell of the cations show a strongly diminished ability to accept hydrogen bonds from other water molecules: the contribution to the θ_{hb} value from accepted hydrogen bonds falls from ~ 0.33 for water molecules that are in the bulk to ~ 0.10 for water molecules that are immediately adjacent to the cations (Figure 6c). This effect appears to be largely independent of the identity of the cation. In contrast, the hydrogen bond donating abilities of waters in the first solvation shell of the cations show a much greater dependence on the identity of the cation (Figure 6d) and are therefore largely responsible for the differences in the total θ_{hb} values shown in Figure 6a. As might be anticipated, there is a gradual decrease in the ability of water molecules in the first solvation shell to donate hydrogen bonds to other water molecules as the cation decreases in size from Cs^+ to Na^+ . When compared with bulk water molecules, however, waters around the larger, less charge-dense cations (Cs^+ , Rb^+ , and K^+) actually show an increased ability to donate hydrogen bonds to neighboring waters; this behavior is consistent with findings obtained by others that these ions behave in some respects more like hydrophobic spheres.²² Again, however, the trend abruptly reverses with Li^+ ; in fact, water molecules that are immediately adjacent to Li^+ ions show an ability to donate hydrogen bonds to other water molecules that is identical to that of water molecules in the bulk (see the solid red lines in Figure 6). (It is to be noted that while water–water hydrogen bonding is greatly diminished in those waters that are further removed from the

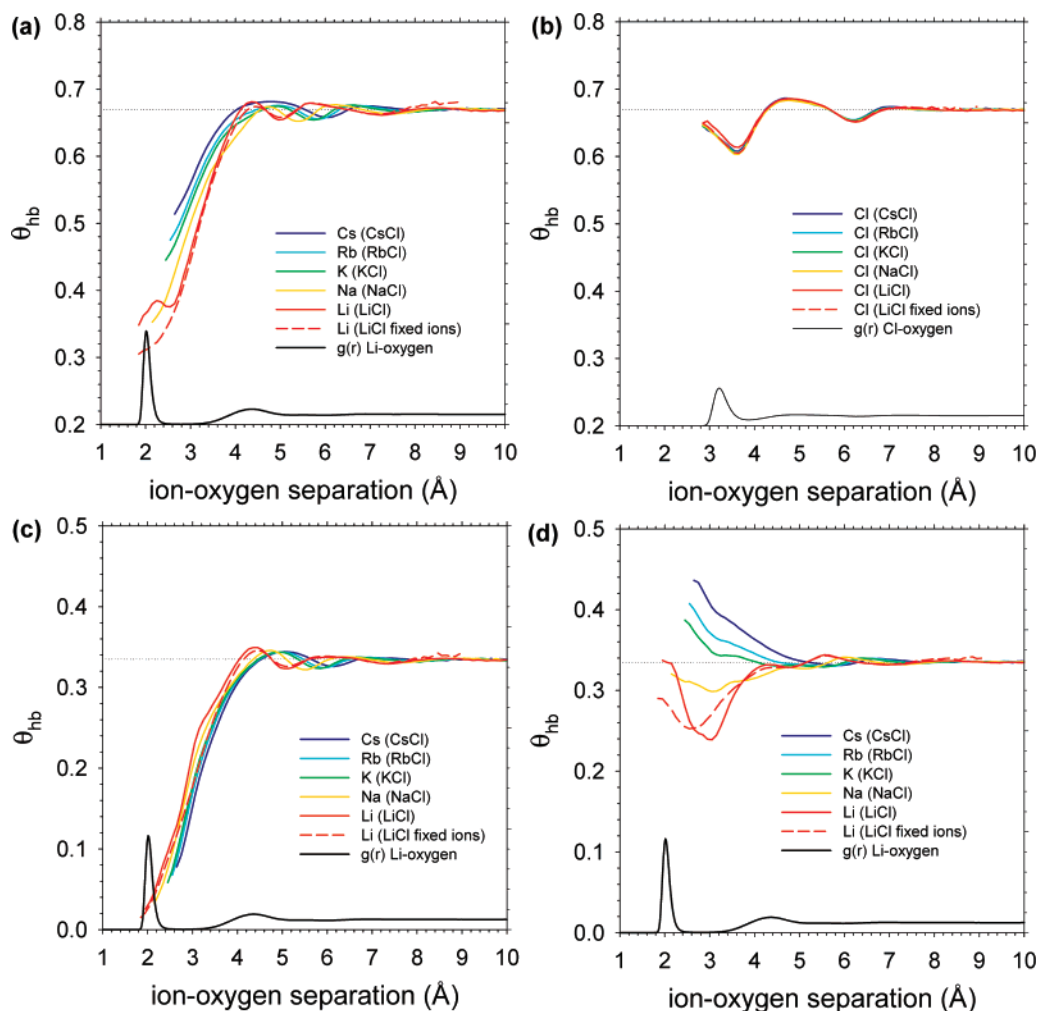


Figure 6. Effects of salts on water–water hydrogen bonding. (a) Mean θ_{hb} of water molecules plotted as a function of their distance from the nearest cation in simulations of Group I cation chloride solutions; (fixed ions denotes the result of a simulation in which ions were prevented from associating by the addition of restraints); for comparison, the Li^+ –water oxygen (RDF) is also plotted at the base of the figure. (b) Mean θ_{hb} of water molecules plotted as a function of their distance from the nearest anion in the same simulations; for comparison, the Cl–water oxygen RDF is plotted at the base of the figure. Panels (c) and (d) show the individual contributions to the mean θ_{hb} values shown in panel (a) due to accepted and donated hydrogen bonds, respectively.

Li^+ surface (2.5–3.5 Å), the number of waters found in this region is very small and therefore makes a negligible contribution to the overall behavior; see the Li^+ –water RDF plotted at the base of this figure.)

Since it has already been noted above that the Li^+ salts tend to form strings with their partner anions, a question that arises is to what extent the unusual water–water hydrogen bonding around Li^+ ions indicated in Figure 6a–d reflects the intrinsic nature of the interaction between Li^+ ions and water and to what extent it is a consequence of the formation of the ionic strings. This question can be answered with the results of additional simulations of the Group I cation chloride salts performed with restraints applied to ensure that all ions remain separated from each other by at least 8 Å. The extent of water–water hydrogen bonding adjacent to Li^+ ions observed in these simulations (dashed red lines in Figures 6–d) is now clearly lower than that adjacent to Na^+ and therefore fits the naïve expectation that water–water hydrogen bonding in the immediate vicinity of an ion should be directly related to the ion’s charge density.¹⁵ Since this result indicates that there is nothing intrinsically unusual about the water–water hydrogen bonding around isolated Li^+ ions, it suggests strongly that the anomalous amount of water–water hydrogen bonding observed around Li^+

ions in unrestrained simulations and the position of Li^+ in the Hofmeister series are both intimately connected to the formation of ionic strings. This conclusion is reinforced by the fact that the θ_{hb} values of the salt solutions obtained from the restrained simulations—in which ion clustering is artificially prevented—no longer correlate so well with the experimental Setchenow constants (Figure 7): linear regression with the computed θ_{hb} values from simulations in which ion clustering is allowed gives $r^2 = 0.702$, while regression with computed θ_{hb} values from simulations in which ion clustering is prevented gives $r^2 = 0.214$.

Discussion

In discussing the above results, the first issue to consider is the quality of the overall correlation between the experimental Setchenow constants and the computed free energies of interaction for the methane–methane and neopentane–neopentane pairs (Figure 1c,d). The fact that a significant correlation is obtained from computed interaction free energies that differ from each other by less than 0.15 kcal/mol (as judged by the range of energies plotted in Figure 1c) demonstrates that 1 μs MD simulations can provide surprisingly precise estimates of association thermodynamics and reinforces a point that we have

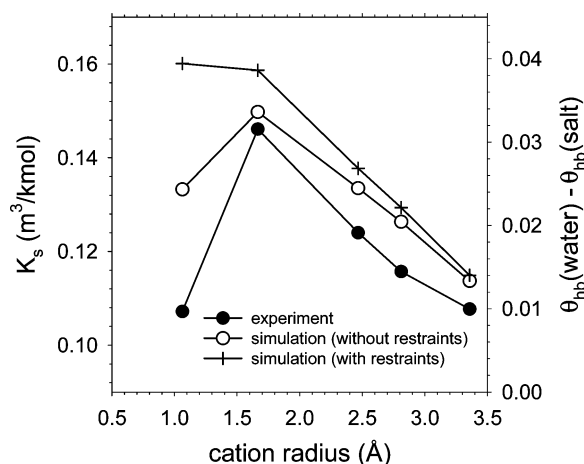


Figure 7. Water–water hydrogen bonding in simulations of Group I cation chloride solutions. Left-hand axis: experimental Setchenow constants (solid circles) plotted vs cation radius; right-hand axis: relative hydrogen bond fraction of water molecules in the same solutions plotted vs cation radius. Results from simulations conducted without restraints are shown as open circles; results from simulations conducted with restraints are shown as crosses.

made elsewhere^{52,69,70} that current computational resources make simple, unforced MD simulations a powerful and general approach to investigating biomolecular association reactions. The fact that the agreement with the experimental Setchenow constants is so good raises another issue: it should be remembered that the potential functions used here are of the simple nonpolarizable variety and were developed many years ago,^{24,25,58,59,62} well before their ability to capture Hofmeister effects could have been assessed. Given the high charge densities of inorganic ions, it is not surprising that a number of simulation studies have suggested that accounting for polarization of coordinating water molecules is likely to be essential for properly describing the behavior of ions in aqueous solution;^{26,35,43} the successful use of potential functions that do not allow for any such polarization effects in the present application may therefore seem surprising. Perhaps the success is due in part to the fact that in considering a hydrophobic association reaction in aqueous solution, a significant cancellation of errors is likely to occur: in particular, the systematic errors inherent in the use of a nonpolarizable treatment of salt ions will (to a first approximation) be as severe when the organic solutes are in a dissociated state as they are when the solutes are in an associated state. For association reactions in which direct binding of ions occurs to one or another of the solutes in either associated or dissociated states, the neglect of explicit polarization effects may be more of a problem. It may also prove to be more of a problem when salts that exert stronger Hofmeister effects (e.g., perchlorate and phosphate) are investigated: it should be remembered that the present studies focus on salts that exert only weak to moderate Hofmeister effects.¹¹

Of course, the present work's reliance on nonpolarizable potentials—which are typically more rapid to compute than comparable polarizable potentials (and much more rapid than ab initio quantum MD approaches, which have recently been applied to study methane–methane association in explicit water)⁷⁶—is to a large extent dictated by the need to perform

very long simulations to obtain statistically converged measures of the free energies of interaction. Performing similar simulations with a polarizable forcefield would be a much more formidable undertaking, although it would be achievable with massively parallel approaches similar to those used to compute very precise estimates of small molecule hydration energies.⁷⁷ In fact, it should be noted that the present set of simulations were themselves of not insignificant expense—a 1 μ s simulation, for example, required on the order of 7 weeks to complete on a single 3GHz CPU—and recognition of this issue has therefore made us consider whether the particular question being studied here, the role of Hofmeister effects, might also be addressable using somewhat simpler and less computationally expensive approaches.

We have identified two possible approaches. The first involves use of the PI formalism, which has been shown here to provide quantitative correlations with the effects of different salts on the computed free energies of interaction for both methane–methane and neopentane–neopentane pairs (Figure 2d). The advantage of the PI formalism in the present context lies in the fact that its application requires only that comparatively short, independent simulations of the associated and dissociated states of the solutes be performed. Such simulations would only need to be run for a period of time sufficient for equilibration of the salt ions' positions around the solutes to be achieved: there would, in particular, be no need to run simulations long enough (e.g., 1 μ s) that equilibration of the actual solute–solute binding interaction occurs.

A second possible approach to predicting or rationalizing the Hofmeister effects of different salts that we have identified here is even simpler: a simulation of the pure salt solution is performed, and the extent of water–water hydrogen bonding in the solution is assessed using the simple measure θ_{hb} . The fact that this latter approach works so well is significant not only from the point of view of identifying a more rapid way of studying Hofmeister effects computationally, but it is also important in that it suggests that the effects themselves can—to a large extent—be understood without considering the solutes themselves. In some respects, this is an expected result: Setchenow constants derived from solubility studies of quite different solutes are usually highly correlated with one another, which indicates that the identity of the solute is of secondary importance in determining their sensitivity to the presence of salts (and consistent with this, the regression studies of Schumpe invoke only an additive constant to account for differences in solutes).¹¹

In another sense, however, the result has a greater significance: it identifies changes in the extent of water–water hydrogen bonding, as measured by θ_{hb} (or the water oxygen–hydrogen RDF), as being intimately connected to the observed Hofmeister effect. Perhaps this issue should not be overemphasized: although we have identified a strong correlation between water structuring and Hofmeister effect, we have not established a causal relationship between the two quantities. It may therefore be that other properties of the system may also be found to serve equally well as predictors of the Hofmeister effect, in much the same way that other experimentally observable properties of solutions (such as surface tension) have been linked to

(76) Li, J.-L.; Car, R.; Tang, C.; Wingreen, N. S. *Proc. Natl. Acad. Sci. U.S.A.* **2007**, *104*, 2626–2630.

(77) Shirts, M. R.; Pitera, J. W.; Swope, W. C.; Pande, V. S. *J. Chem. Phys.* **2003**, *119*, 5740–5761.

solubility effects.¹⁴ The advantages of θ_{hb} —at least as a simulation observable—are, however, two-fold. First, θ_{hb} serves as a straightforward measure of the effect of a salt on the overall behavior of the waters constituting the solution. Second, since it can be computed as a single number for individual water molecules—in a way that an RDF cannot—it can be used straightforwardly to analyze and compare the behaviors of waters in different environments of interest. This second advantage has been heavily exploited in the analyses presented in Figure 6 showing how the extent of water–water hydrogen bonding varies with distance from nearby ions.

It is notable that the major simulation properties that have been examined here (i.e., the changes in the computed free energies of interaction), the $\Delta\Gamma_{\text{salt}}$ values obtained from application of the PI formalism, and the θ_{hb} values of water molecules computed from pure salt solution simulations, are all successful in capturing the anomalous behavior of Li^+ ions. To our knowledge, this is the first time that the strengths of hydrophobic solute–solute interactions in lithium salts have been directly computed; the fact that Li^+ 's unusual behavior relative to other Group I salts can be successfully captured by such simulations further reinforces the general statement made previously concerning the utility of nonpolarizable potential functions. The fact that a similarly good correlation with Li^+ 's experimental Setchenow constant can also be obtained using the more indirect θ_{hb} measure, however, is perhaps equally significant: it indicates that lithium's anomalous Hofmeister behavior is not a result of any unusual direct interactions between Li^+ ions and hydrophobic solutes but must instead be a result of the effects of Li^+ ions on the solvent.

The crucial factor in this ability to correctly describe the Hofmeister properties of lithium salt solutions appears to be the formation, during the simulations, of linear strings of alternating Li^+ and halide ions. This finding almost certainly explains why a previous simulation study that focused on the extent of water structuring in a system containing only a single, isolated ion was unable to explain lithium's anomalous salting-out behavior;¹⁵ consistent with the latter study, we are similarly unable to explain the anomalous behavior using simulations in which string formation is artificially prevented (Figure 7). These findings also demonstrate that to fully understand the experimentally observed behavior of a salt solution, it is necessary to simulate the actual salt solution rather than its isolated, component ions, and on a time scale sufficient that a thorough sampling of the salt ions' behavior is achieved: it is important to note, for example, that significant string formation did not occur in the present MD simulations until more than 10–20 ns had elapsed.

Since the formation of linear ion strings is somewhat surprising, it is worth noting that they have also been observed by others in slightly different contexts^{31,78–80} and in two additional sets of simulations that we have performed: (a) a 1 M LiBr solution employing a simulation box of 8 times the original volume (Table 3 in the Supporting Information) and (b) a 1 M LiCl solution simulated with a recently published, updated set of ion parameters³⁷ (data not shown). Although none

of these observations proves conclusively that such strings are not a simulation artifact, they do argue that their formation is at least a relatively robust prediction of the simulation methods. While it is difficult, if not impossible, to establish the cause of string formation, it is interesting to note that the water molecules that coordinate Li^+ ions in strings show an ability to donate hydrogen bonds to other water molecules that is essentially identical to that of water molecules in bulk solution (Figure 6d); perhaps, therefore, string formation is driven by a tendency to minimize the thermodynamic perturbation of a water structure that would otherwise be caused by the presence of dissolved salts. Regardless of what the driving force for their formation is, the key point that emerges is that it is the formation of strings that provides a compelling, potential explanation for lithium's anomalous Hofmeister behavior. If the existence of such strings could be verified experimentally, it would provide a powerful demonstration of the utility of currently available simulation methods for uncovering unanticipated atomic-scale phenomena that drive molecular interactions.

Conclusion

In this work, we have shown that very long (1 μs) simulations of the unbiased association of pairs of hydrophobic molecules in different salt solutions can reproduce experimentally observed Hofmeister trends. We have shown excellent agreement between changes in the preferential interaction coefficients ($\Delta\Gamma_{\text{salt}}$) upon hydrophobic association and the effect of salts on the strength of hydrophobic interactions. Given that efforts to understand the Hofmeister effects of salts often focus exclusively on the interaction between the salt and the hydrophobic solute (e.g., ref 48), it is important to note that we have been able to show here that quantitative predictions of the Hofmeister effects can be made simply by measuring the hydrogen bond ratio θ_{hb} from simulations of pure salt solutions without any hydrophobic solutes. This key result suggests that the change in water structure due to the addition of salt may be more fundamental to the Hofmeister effects of simple salts than preferential interactions between salt and hydrophobic solutes.

An important potential advantage of theoretical methods is their ability to capture and explain anomalous experimental observations. In this work, we provide an example of this by showing that molecular simulations can accurately describe the anomalously low (and previously unexplained¹⁵) Setchenow constants of lithium salts; based on additional simulations (Figure 7), we have shown that it is the unexpected formation of linear strings of ions that appear to be the cause of this anomalous behavior. These results and predictions should be amenable to experimental testing via modern spectroscopic and scattering techniques.

Acknowledgment. We are grateful to Bret Freudenthal for fruitful discussions during the early stages of this work and to the anonymous reviewers for insightful comments and suggestions. This work was supported in part by a CAREER award to A.H.E. from the National Science Foundation.

Supporting Information Available: Partial charges assigned to alkyl ammonium cations; correlations between experimental Setchenow constants and computed Γ_{salt} values for hydrophobic solutes in the dissociated state; effects of salt on the computed interaction free energies at all inter-solute separations for the

(78) Georgalis, Y.; Kierzek, A. M.; Saenger, W. *J. Phys. Chem. B* **2000**, *104*, 3405–3406.

(79) Mason, P. E.; Dempsey, C. E.; Neilson, G. W.; Brady, J. W. *J. Phys. Chem. B* **2005**, *109*, 24185–24196.

(80) Chen, A. A.; Pappu, R. V. *J. Phys. Chem. B* **2007**, *111*, 6469–6478.

methane–methane and neopentane–neopentane interactions; correlations between experimental Setchenow constants and computed $\Delta\Gamma_{\text{salt}}$ values for different choices of the cutoff distance; changes in water oxygen–oxygen RDFs with correlations to Setchenow constants; changes in water oxygen–hydrogen RDFs with correlations to Setchenow constants; θ_{hb} values plotted as a function of distance from methane in the eight salt solutions with correlations to Setchenow constants and mean θ_{hb} values computed from simulations of pure salt

solutions and salt solutions with two dissolved methanes; θ_{hb} values plotted as a function of distance from the nearest ion for different sodium salts; Γ_{salt} and $\Delta\Gamma_{\text{salt}}$ values with variable cutoff distances; θ_{hb} values and Setchenow constants for all salt solutions studied; and ion clustering data. This material is available free of charge via the Internet at <http://pubs.acs.org>.

JA073097Z